

Rational approximation of the Ernst equation for dual angle R1 mapping revisited: beyond the small flip-angle assumption

Luke J. Edwards¹, Kerrin J. Pine¹, Gunther Helms²,
Nikolaus Weiskopf^{1,3}

¹Department of Neurophysics, Max Planck Institute for Human Cognitive and Brain Sciences,
Leipzig, Germany

²Medical Radiation Physics, Clinical Sciences Lund, Lund University, Lund, Sweden

³Felix Bloch Institute for Solid State Physics, Faculty of Physics and Earth Sciences,
Leipzig University, Germany

June 8, 2021

Introduction

Dual flip angle R1 mapping – collecting two FLASH volumes with different flip angles (α_1 and α_2) and (potentially) different repetition times (TR1 and TR2) – is a workhorse of proton density (PD) and R1 mapping in the in vivo human brain [1]. An efficient method for computing R1 and PD from the two volumes, implemented in the hMRI toolbox (hmri.info), uses a rational approximation of the Ernst equation derived under the assumption of short TR and small α [1, 2]. However, the assumption of small α can break down at 7T, where B1 inhomogeneities are large [3]. Here we present and validate a modified rational approximation that is valid even for large α .

Methods

The derivation is presented in Fig. 1. First, we make a half-angle tangent substitution into the Ernst equation (Eq. (1)) to simplify the trigonometric functions of α without approximation (Eq. (4)) [4]. We then make the assumption TR is small such that R1 TR is small. Because the Ernst equation is a rational function, we use rational Padé approximants [5] to expand around TR = 0, then solve for R1 and PD.

We tested the method in simulations and on a 7T in vivo dataset. To demonstrate that the result is non-obvious, the simulations also compared the result of simply inserting the linear expansion of $\exp(-R1 \text{ TR})$ into Eq. (4).

Results and discussion

Fig. 2 shows the benefits of the novel approximation for a simulated 7T acquisition. Fig. 3 shows these benefits also extend to a typical experimental dataset.

Formally, our result is the specific dual-angle case of an N flip angle result suggested (but not evaluated) in [6]. The left panel of Fig. 2 shows that it is important to always evaluate the numerical accuracy of such results, as substituting linear approximations into rational functions is not guaranteed to give good results.

We retained the assumption of short TR. While a closed form exact solution without approximation is possible when $TR_1 = TR_2$ [4], this is not generally applicable. Nonlinear fitting can be used to estimate R1 and PD from Eq. (1), but will be very slow.

We omitted magnetization transfer and imperfect spoiling in our analysis, which also increase with increasing flip angle [7, 8]. However, Fig. 3 implies that our method still removes a significant amount of bias.

This method has been implemented into the hMRI toolbox (hmri.info) and will be included in an upcoming release. This will allow others to efficiently extract more precise R1 estimates.

References

- [1] K. Tabelow et al. *Neuroimage*, 2019.
- [2] G. Helms et al. *Magn. Reson. Med.*, 2008. Erratum: *Magn. Reson. Med.* 63:1136 (2010).
- [3] A. Lutti et al. *PLOS ONE*, 2012.
- [4] H. Dathe and G. Helms. *Phys. Med. Biol.*, 2010.
- [5] W. H. Press et al. *Numerical Recipes in C++: The Art of Scientific Computing*. 2002.
- [6] G. Helms et al. *Magn. Reson. Med.*, 2011.
- [7] A. G. Teixeira et al. *Magn. Reson. Med.*, 2019.
- [8] N. Corbin and M. F. Callaghan. *Magn. Reson. Med.*, 2021.

Starting from the Ernst equation

$$S(\alpha, \text{TR}) = \text{PD} \sin(\alpha) \frac{1 - \exp(-\text{R1 TR})}{1 - \cos(\alpha) \exp(-\text{R1 TR})} \quad (1)$$

we follow [4] in making half-angle tangent substitutions using the identities

$$\sin(\alpha) = \frac{\tau}{1 + (\tau/2)^2}; \quad \cos(\alpha) = \frac{1 - (\tau/2)^2}{1 + (\tau/2)^2} \quad (2)$$

where

$$\tau = 2 \tan(\alpha/2) \quad (3)$$

to give

$$S(\tau, \text{TR}) = \text{PD} \tau \frac{1 - \exp(-\text{R1 TR})}{1 - \exp(-\text{R1 TR}) + (\tau/2)^2(1 + \exp(-\text{R1 TR}))}, \quad (4)$$

which is equivalent to Eq. (5) in [4].

The [1/1] Padé approximant [5] of Eq. (4) around $\text{R1 TR} = 0$ is:

$$S(\tau, \text{TR}) \approx \text{PD} \tau \frac{\text{R1 TR}}{\tau^2/2 + \text{R1 TR}}. \quad (5)$$

The left panel of Fig. 2 shows that Eq. (5) gives a good approximation of the signal. Note that Eq. (5) differs from the result of simply inserting $\exp(-\text{R1 TR}) \approx 1 - \text{R1 TR}$ into Eq. (4), which does not approximate the signal well (Fig. 2).

Eq. (5) has the same form as the small angle approximation result Eq. (A.5) in [1] (with τ instead of α), so we can immediately write our final result

$$\text{R1} \approx \frac{1}{2} \frac{(S_1 \tau_1 / \text{TR1}) - (S_2 \tau_2 / \text{TR2})}{(S_2 / \tau_2) - (S_1 / \tau_1)} \quad (6)$$

and

$$\text{PD} \approx S_2 S_1 \frac{(\text{TR2} \tau_1 / \tau_2) - (\text{TR1} \tau_2 / \tau_1)}{S_1 \text{TR2} \tau_1 - S_2 \text{TR1} \tau_2} \quad (7)$$

from Eqs. (A.6) and (A.7) in [1].

Figure 1: Derivation of the [1/1] Padé rational approximation and solution for a dual flip-angle experiment.

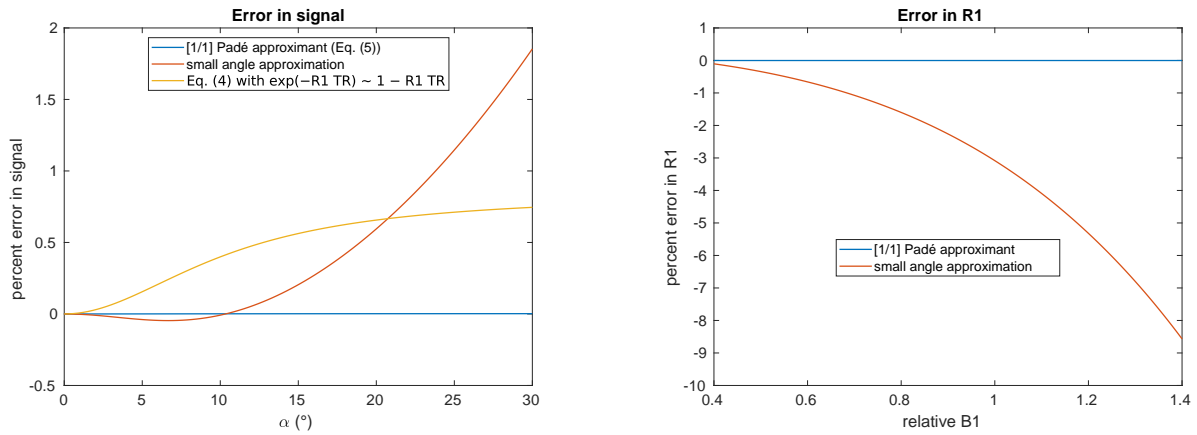


Figure 2: Relative errors in approximations from simulations. Data simulated using the Ernst equation (Eq. (1)) and typical 7T parameters: $TR = 23.5$ ms, $R1 = 0.7$ s $^{-1}$. For simplicity, $PD = 1$. Left: Errors in the signal grow large when using either the small angle approximation or expansion of the exponentials in Eq. (4), but remain close to zero for the Padé approximant (Eq. (5)), showing that the Padé approximant is numerically better behaved. Right: Errors in the signal correspond to errors in $R1$ estimates which scale with $B1$ inhomogeneity. Nominal flip angles: $\alpha_1 = 8^\circ$, $\alpha_2 = 28^\circ$. Flip angles were chosen to be close to optimal for estimation of $R1$ following [4]. The $B1$ range covers a typical range in human brain at 7T. Because the third signal model gave a poor representation of the signal (left panel), it is omitted in the right panel.

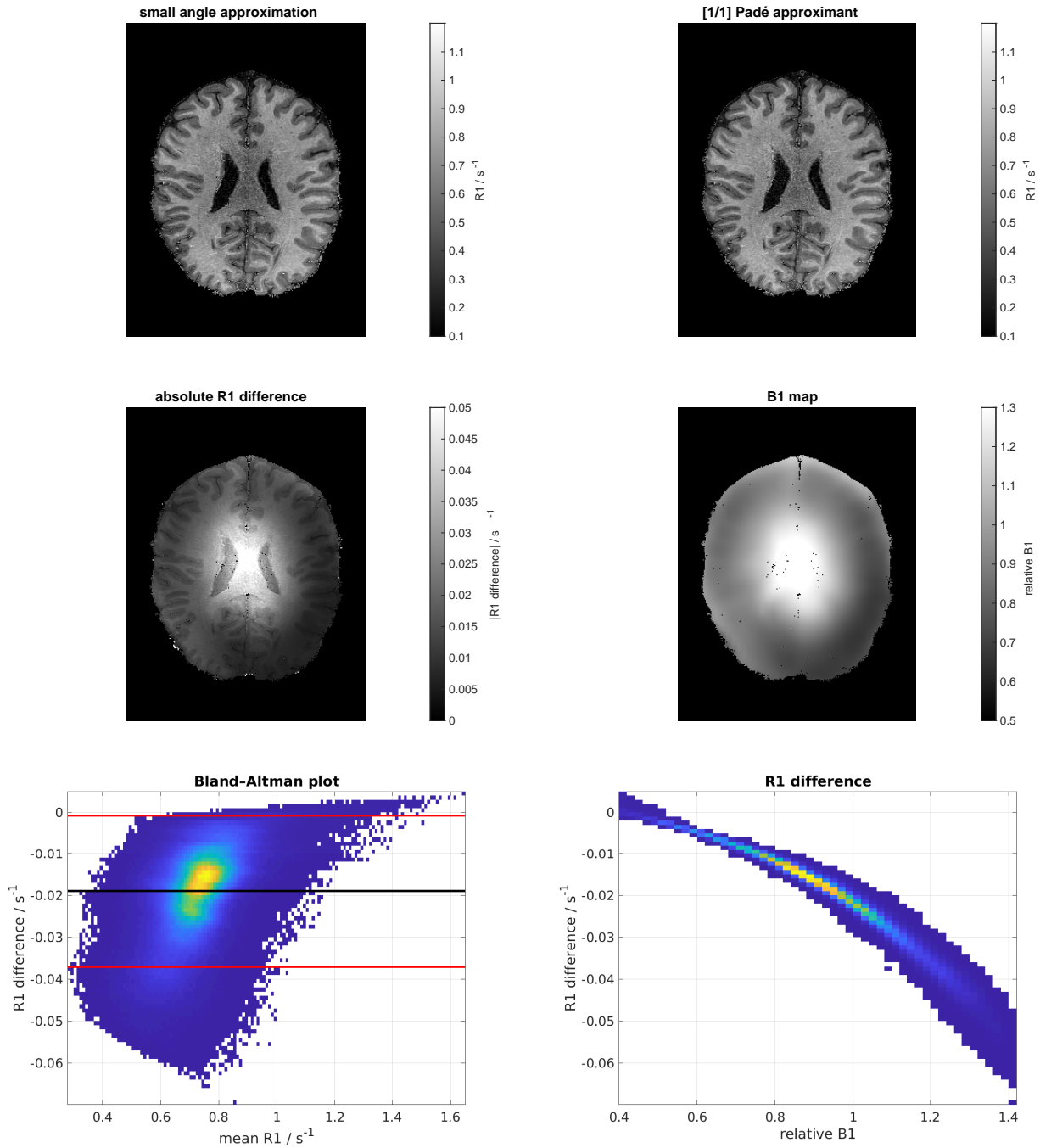


Figure 3: In vivo results. The subject gave written informed consent before scanning. Parameters: Siemens Terra 7T MRI scanner, 0.65 mm isotropic resolution FLASH acquisitions, $TR = 23.5$ ms, 6 equispaced TEs 2.8–14.3 ms, nominal $\alpha_1 = 8^\circ$, $\alpha_2 = 28^\circ$, B1 inhomogeneity corrected using a SE/STE-EPI B1 map [3]. R1 and PD estimated with the hMRI toolbox [1] and a version modified to use Eq. (6). The R1 maps are superficially similar (top row), but their difference (middle-left) shows a pattern reflecting B1 inhomogeneity (middle-right; interpolated to R1 space). The Bland–Altman plot of R1 over a white matter mask (bottom-left) shows the small-angle approximation is biased relative to the Padé approximant (black line: mean difference, red lines: mean difference ± 1.96 standard deviations of the difference). Plotted as a function of B1 (bottom-right), we see that the white matter R1 estimates follow the theoretical prediction of Fig. 2.